Microwave Review
December 2024, Vol. 30, No. 2, pp. 23-35
DOI: 10.18485/mtts_mr.2024.30.2.3

Lotus-Shaped Triple-Tuned Antenna with SRR Quadruplets for SDARS and Weather RADAR

Sanjay Singh[1], Vipul Sharma[1], Narinder Sharma[2], Atul Varshney[1]

Abstract – **The article presents the design and investigation of a lotus-shaped triple-tuned wideband monopole-antenna for wireless communication services (WCS), satellite radio, and weather RADAR applications. The novel lotus-shaped antenna structure contains seven arms developed using arithmetic operations and loaded with SRR-quadruplets. Further, the effect of ring orientation position changes is analysed. Seven arms increase the electrical length of the patch which yields an improvement in broad bandwidth. The parasitic loading of an antenna with SRR quadruplets changes the nature of the antenna to triple-tuned at 2.04 GHz, 2.27 GHz, and 2.90 GHz with enhanced -10dB fractional bandwidth (FBW) 57.19% from initially designed single band (2.06-3.12 GHz) antenna. A wideband is achieved by reduced compressed ground. The proposed antenna achieves a peak gain of 5.2dBi and an efficiency of 92%. The RLC equivalent circuit of the designed antenna is presented for compatibility at low-frequency operations. The ADS and HFSS-generated electrical equivalent circuit reflection coefficients are found in excellent agreements and they validate the antenna. The wideband nature of the antenna from 1.61GHz to 3.24 GHz makes this antenna suitable for WCS, satellite digital audio radio services (SDARS), and weather RADAR applications. The modified antenna structure and quadruplet-SRR loading offer additional 5G bands, GSM, and PCS applications.**

Keywords – **ISM, Parasitic Loading, Relocated SRRs, SDAR, SRR quadruplets, WCS, Wideband, Wi-Fi.**

I. INTRODUCTION

In the present era, the antenna is a key element for all wireless communication to receive/transmit RF energy. In modern planar technology like microwave monolithic Integrated circuits (MMIC) and Monolithic Integrated Circuits (MIC) circuits and devices, the antenna is used for RF energy launcher in the microstrip to waveguide transitions, dielectric resonator antennas, substrate-integrated waveguide transitions, Microwave devices as RF signal excitation, etc [1-5]. The current planar antenna technology research involves multiple-input multiple-output (MIMO), Massive MIMO, frequency/pattern/polarization reconfigurable, fractal, metamaterial, frequency selective surfaces, resistive interface surfaces, electromagnetic bandgaps, etc for the improvement in the gain enhancement, to widen in bandwidth, more application coverage, defected ground technology, etc [6-11]. The metamaterial and fractal technology jointly play a magical role as an alternative for the antenna resultant parameter and radiation characteristics improvement/alterations [12-14]. With the rapid advances in the field of IoT technology, almost all applications are being used in the different fields of tracking, sensing, security, agriculture, smart homes and cities, unmanned machines, body health analysis, gaming technology, smart tools handling modems (Federal Communications Commission) [15].

Literature Review: The most ordinary exercise of the WCS spectrum is mobile voice and data services, including cell phones, text messaging, and the Internet. In the United States the 2305–2360 MHz band is divided between cellular networks and satellite radio (SDARS) users, the SDARS spectrum allocation, which is 2320–2345 MHz [15]. Elavarasi et al., have developed a compact CPW-fed, leaf-shaped Koch fractal multiband antenna loaded with a single unit of SRR for HIPERLAN, and L-band to K-band applications. The fabricated antenna is economical (FR-4 substrate) while it has complex patch geometry and a low peak gain of 3.9 dBi [12]. Sharma et al., have proposed an octagonal-shaped CSRR and C-slotted monopole low-cost and compact antenna for UWB (2.94-12GHz) applications with Wi-MAX and WLAN band rejection capabilities with a peak gain of 6.75dBi and radiation efficiency above 85.54%. The added slots make the fabrication difficult [13]. Varshney et al., have presented a fan-shaped tri-arm monopole antenna for ISM and PCS band applications. The antenna is parasitically loaded with SRR triplets to improve the gain and maintain the wideband performance. The antenna structure was simple, and economical while the added outside three arms increased the electrical length/periphery that demands additional patch area [16]. Further, Varshney et al., have modified the circular patch monopole antenna with windmill-shaped tri-arms and loaded with CSRR in the patch center for notch band elimination. This makes the antenna most suitable for ISM and PCS applications but again the added slot in the patch increases the fabrication difficulties [2]. Zambak et al., have proposed a compact L-shaped antenna for ISM-band and IoT applications. The antenna has a simple structure and excellent radiation efficiency of 98% with a low gain of 2.09 dBi [17]. Ghaffar et al., have designed an isosceles-slotted triangular-shaped frequency reconfigurable multi-mode antenna for ISM, 5G Sub 6 GHz, and S-band applications using PIN diodes as switching elements for four modes of operations. The modified triangular-shaped antenna was developed from a rectangular patch without using SRR loading [18]. Ullah, et al., have developed a super wideband, offset-fed modified S-

Article history: Received March 04, 2024; Accepted April 11, 2024.

[1]Sanjay Singh, Vipul Sharma, and Atul Varshney are with the Electronic Engineering Department at Faculty of Engineering & Technology, Gurkula Kangri (Deemed to be) University, Haridwar, Uttarakhand, India. E-mail: sanjaysingh89ind@gmail.com, vipul.s@rediffmail.com, atulgkvright@gmail.com

[2]Narinder Sharma is with the Department of Electronics and Communication Engineering of Amritsar College of Engineering and Technology, Amritsar, Punjab, India E-mail: dr.narinder.sharma0209@gmail.com

Shaped (meandered line-based) monopole antenna using the defective ground for WLAN, ISM, WiMAX, UWB, and WCS applications. Antenna geometry is simple, easy to fabricate, and covers a super wideband range of frequencies 3.08 GHz to 40.9 GHz but it is costlier. The antenna achieves a peak gain of 5.9 dBi and a radiation efficiency of 92.7% [19]. Mansouri et al., have reported two CPW-fed multi-notch band circular monopole antennas using L-shaped without vias and U-shaped stubs with vias at the bottom surface for WLAN, Hyper-LAN, and Wi-Max applications. Further, Mansouri et al., have designed and fabricated a quarter-wave transformer-fed tri-arm lotus-shaped monopole antenna. This will result in UWB bandwidth ranging from 1.42 GHz to 10 GHz [20]. Fonseca et al., have designed an in set-fed symmetrically located double Koch (third iteration) slotted rectangular patch antenna for X-band and military applications. Antenna reports quad-band reflection coefficients with low radiation efficiency and directional radiation patterns again slots increase fabrication difficulties [21]. Sharma et al., have fabricated a rectangular patch antenna loaded with a Split ring in the ground for Wi-Max (2.5-2.7 GHz), WLAN (2.4-2.48 GHz), Bluetooth (2.4-2.48 GHz), and 4G-LTE (2.3-2.4 GHz) application. The antenna structure is very simple with a peak gain of 4.07 dBi and radiation efficiency of 96.2% [22]. Rahman et al. have fabricated and measured a human Skulled-shaped, defective compressed ground monopole planar antenna at 3 GHz for super wideband applications from 3.0 GHz to 27.5 GHz. The antenna achieves a gain of 6.3 dBi and a high radiation efficiency of 93%. The antenna is costly as it is fabricated on the Roger RT Duroid substrate. The defective compressed ground helps to widen the FBW [23]. Varshney et al., have realized a frequency-reconfigurable dodecagon-shaped monopole antenna loaded with tri-triangular arms using four PIN diodes, BAR 6402V for 8 switching modes. Antenna design is complex and costlier because of the presence of the four PIN diodes. The antenna is most suitable for ISM and WCS applications [24]. Antony and Dasgupta have fabricated a tri-arm lotus-shaped circular slotted coplanar (CPW)-fed ultra-wideband (UWB) antenna ranging from 2.0 GHz to 11.8 GHz. When the antenna is loaded with double layered square and circular-shaped frequency selective surface (FSS) layer combination of 25-unit cells, then it will cover a band of 3.8 GHz to14.4 GHz (FBW 116%) with a peak gain of 5.9 dBi. The patch was developed from a circular patch [25]. Sudarshan et al., have designed a CPW-fed UWB three arms lotus-shaped antenna from a combination of semicircular and triangular shapes. The antenna results in an FBW of 132% from 2.86-14.0 GHz with a peak gain of 5.3 dBi [26]. Samsuzzaman et al., have fabricated and tested a lotus-shaped edge-fed monopole dual-band antenna for Bluetooth and UWB applications. It covers a bandwidth of 2.3 to 2.6 GHz and 3.3 to 12 GHz with a peak gain of 6.2 dBi [27].

Research Gap: The above researchers did not use SRRs for improvements of the bandwidth and maintaining the gain also the number of the lotus arms is limited to three numbers or less [20, 25, 26, 27]. The applications covered by the aforementioned lotus-shaped antennas are above 2.3GHz and limited to 14.4GHz. The outer appended triangular and rectangular arms increase the patch area [14, 24, 33]. Similar special-shaped antennas are compared in Table I to extract the research gap. The proposed antenna utilizes the SRRs and also covers lower band applications from 1.61 GHz to 3.24 GHz like GSM, CDMA, ISM, Bluetooth, WLAN, Wi-Max, 5G bands, SDARS, WCS, PCS, DSC, etc.

TABLE 1
NOVELTY TABLE

Ref no.	BW (GHz)	SRR used	Size (mm^3)	RLC Equ. Circuit	Application
[9]	(UWB) (3.8–14.4)	SRR is not used. Uses FSS	31× 30× 1.8	Not given	C, X, and partially Ku bands
[20]	UWB (1.42–10)	NO	50× 43× 1.6	Not given	L-band, C-band, and X-bands
[22]	UWB (2.3–2.6) and (3.3–12)	NO	44× 42× 1.6	Not given	Bluetooth and UWB without interference between each other
This work	Wide band (1.61-3.24)	Yes, 4-SRR	44× 40× 1.6	Given	GSM, CDMA, ISM, Bluetooth, WLAN, Wi-Max, 5G bands, SDARS, WCS, PCS, DSC etc.

Research Objectives: Keeping these research gaps in mind a polynomial shape is etched from the rectangular patch to get the desired shape without enhancing the patch area. Therefore, a new type of antenna is needed to cover applications below 2.3 GHz and also cover applications above 2.3 GHz. The following research objectives have been made from the related literature research gap studies;

- The primary objective of this study is to design the simplest, slotless, low-cost, compact planar antenna with a wide bandwidth that works well between 1.5 GHz to 3.5 GHz range with acceptable gains [14].

-Another objective of this research is to make a low-profile, simple, easy-to-fabricate novel modified-rectangular special-shaped nature-inspired monopole antennas with multi-arms for wideband, multi-tuned operations [8, 18].

-The further aim of this work is to load the special-shaped modified rectangular patch antenna with split ring resonators (SRRs) in monopole ground to make the wideband for multiple resonance frequencies [12,14]. Also, investigate the effect of the orientations of the SRR rings.

- The additional aim of this work is to generate the RLC electrical equivalent circuit for the proposed antenna as well as their validation using ADS software [2, 4, 5, 14, 16].

Novelty and Contributions: The proposed antenna in this article is an extension of the special-shaped antenna as it is developed by a novel technique instead of standard fractal iterations and order rules [28, 29]. The contribution of this proposed antenna is the parasitic loading of SRR-quadruplets changes the behavior of the antenna from single-tuned to triple-tuned. This work also includes the effect of the orientations of the rings of the four SRRs. The changes in the

SRR ring-cut orientations were also analyzed. These changes improve the reflection coefficients and enhance the fractional bandwidth by maintaining the peak gain values and their efficiencies. The generation of RLC electrical equivalent circuits and their validation is also another novelty of this conducted research.

The research paper presents a low-cost, triple-tuned, wideband, special-shaped radiating patch with seven fractal arms lotus-shaped, nature-inspired antenna design development, parametric study, fabrication, testing, and analysis of the resultant parameters in terms of reflection coefficients, FBW, Antenna gain, radiation patterns, and electrical equivalent circuits. Finally, the paper concludes with the proposed antenna's future scope.

II. Material and Methodology

The antenna is developed from the rectangular patch antenna by subtracting the closed polynomial fractal at a frequency of 2.85 GHz on a low-profile FR4 substrate. The modified rectangular patch lotus-shaped, parasitically loaded with four SRR, compact, low-profile antenna is designed at a frequency (f_o) of 2.85 GHz on a piece of FR-4 substrate of size 44mm × 40mm with permittivity (ε_r), 4.4 GHz, and thickness (h) of 1.6mm.

A. Antenna Design Geometry and Dimensions

TABLE 2
LOTUS-SHAPED ANTENNA DIMENSIONS

Antenna Dimension	Dimension Designation	Design Dimensions (mm)
Substrate Width	*W_sub*	44.0
Substrate Length	*L_sub*	40.0
Substrate Thickness	*H*	1.6
Patch Width	*W_P*	32
Patch Length	*L_P*	24.7
Feed Width	*W_f*	3.06
Feed Length	*L_f*	13.9584
Dimensions of Symmetric Half-sided Lotus Leaves	*a_1*	15.2575
------same as above------	*a_2*	16.7324
------same as above------	*a_3*	15.0416
------same as above------	*a_4*	9.39415
------same as above------	*a_5*	11.9152
------same as above------	*a_6*	11.3412
------same as above------	*a_7*	8.0388
Compressed Ground Width	*W_gnd*	33
Reduced Ground Length	*L_gnd*	7.5
Width of Split Rings	*w=g*	0.50
SRR cut	*G*	0.50
The gap between Split Rings	*D*	1.0
First Outer ring radius	*R_1ext*	4.854
second Outer ring radius	*R_2ext=R_1ext-w*	4.354
First Inner ring radius	*R_1int=R_2ext-d*	3.354
second Inner ring radius	*R_2int=R_1int-w*	2.854
SRR rings orientations	----------	Out of phase,180°
SRR center locations	*O*1 (x, y, z)	

The antenna patch dimensions are evaluated from the fundamental rectangular patch antenna equations [29, 30]. The seven arms lotus-shaped antenna main patch is developed by subtracting a polynomial shape from the standard rectangular patch antenna designed at a frequency of 2.85GHz. This results in a special-shaped novel geometry as represented in Fig. 1 (a-d). Each SRR dimension is evaluated at a frequency of 2.85 GHz [31, 32]. All the proposed antenna dimensions are arranged in Table 2.

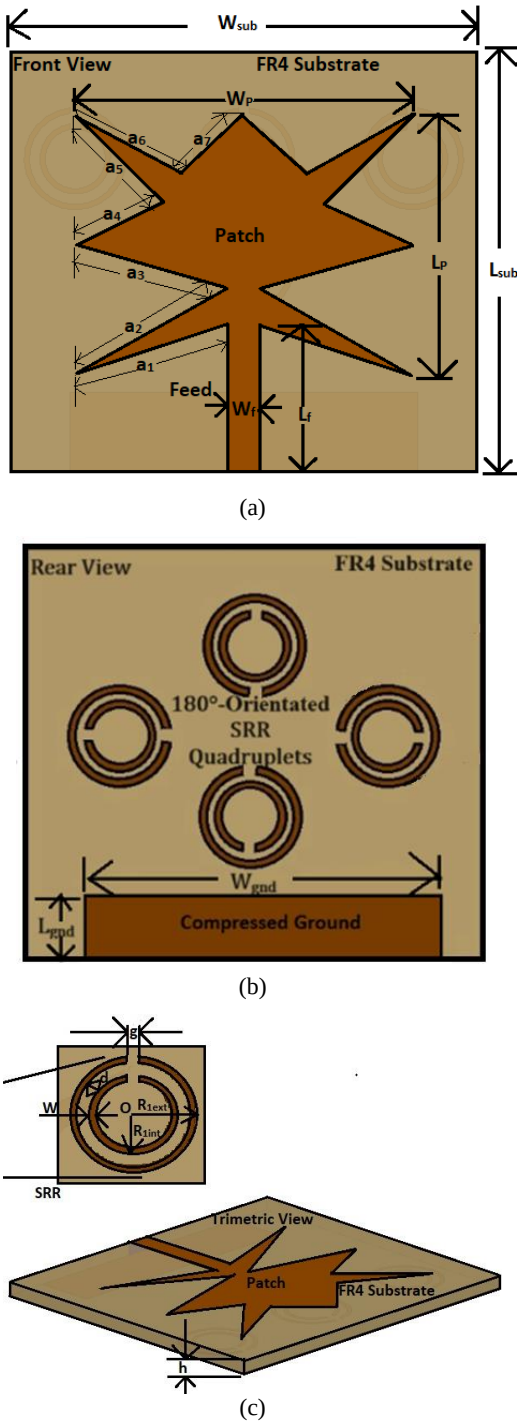

Fig. 1. Antenna Geometry: (a) Front View, (b) Rear View and (c) Trimetric View

B. A Journey of Rectangular Patch to Lotus-Shaped Patch Monopole Antenna

Rationale of Patch-shape Generation from Rectangular patch: The previously existing literature based on lotus shaped antennas are not exactly provides exact lotus shaped antenna. These are developed from the circle and rectangular/triangular shapes combinations [9, 20, 22]. In the proposed article a new method has been presented to generate an irregular patch (lotus shaped) tri-band antenna.

The proposed lotus shaped antenna is developed from a fundamental edge-fed rectangular microstrip patch antenna of design-1 as shown in Fig. 2(a). The ground size is reduced to achieve wideband performance as shown in Fig. 2(b). Still reduced ground does not result in a reflection coefficient lower than -10dB. Therefore, the patch of the antenna is fractalized with a polyline closed symmetrical shape to achieve a reflection coefficient lower than -10dB. This results monopole lotus-shaped antenna as represented in Fig. 2(c). This results in wideband performance with a fractional bandwidth (FBW) of 33.89% and improved radiation efficiency of 93%. Further improvement in the wideband FBW is achieved by compressing the reduced ground width symmetrically around the feed as displayed in Fig. 2(d). This results in about a 3% improvement in FBW with a slight reduction in antenna gain value. The reduced value of the gain is further improved by parasitic loading of the ground plane with SRR quadruplets at the suitable optimized locations. As displayed in Fig. 2(e). The overall lotus-shaped patch development operations novel idea has been step-by-step illustrated in Fig. 2(f). This will result in the proposed antenna geometry. All the five design steps modifications and developments are summarized in Table 3.

Operations involved in the generation of seven-arm lotus-shaped patch geometry: Initially rectangular patch is designed then the edge feed of the root (conventional) rectangular patch is shifted inside (inset feed) the rectangular patch by 5.3mm to match the impedance. Then a fictitious regular octagon with each arm length equal to 6.58 mm of radius 8.5mm from the middle of a rectangular patch (1 mm up along patch length i.e. 22.47 mm from substrate corner along length axis) was drawn as shown by the dotted line in Fig. 2(f). Then 17 points are chosen on the feed, rectangular patch, and regular octagon. Finally, the extra rectangular patch and fictitious octagon shapes are removed, and then by joining all these points from 1 to 17 the proposed shape of the seven-arm lotus-shaped patch. All the operations involved in the generation of the arms lotus-shaped patch are illustrated in Fig. 2(f). The following major steps are used to develop the lotus shaped antenna;

Step1: Edge feed rectangular patch is designed at 2.85 GHz (Fig. 2(f) first).

Step 2: The impedance matching is achieved by converting edge feed into inset feed with 5.3 mm shifting (Fig. 2(f) second). The arrow head indicates the directions of shifting.

Step 3: An imaginary regular octagon has been plotted inside the rectanglular patch with radius equal to the distance between the centre of rectangular patch and the inner edge centre of the feed width (Fig. 2(f) third).

Step 4: In this step polyline is used to meet the points as indicated in the Fig. 2(f) third, to obtain the required lotus shaped patch. the red lotus dotted lines are used to meet the indicated points on the rectangular patch in sequential manner from 1 to 17.

Step 5: Further, in this step the fictitious octagonal and conventional rectangular patch have been deleted as illustrated in the Fig. 2(f) fourth.

Step 6: Furthermore, in last step the obtained polygon shaped is added with the edge feed as illustrated in the Fig. 2(f) five.

The advantage of doing so provides a novel idea that no need of further impedance matching is required and reduced copper requirement of the patch gives added space for attachment of higher number of passive components in the patch.

TABLE 3

ANTENNA DESIGN DEVELOPMENT FROM RECTANGULAR PATCH TO PROPOSED LOTUS-SHAPED FRACTAL ANTENNA

Antenna Design Development	Reson. Freq., f_r (GHz)	Ref. Coeff., S_{11} (dB)	Band (GHz)	-10 dB FBW (%)	Gain (dBi)	Rad. Eff. (%)
Rectangular Patch with Full Ground	2.77	-7.45	Not Present	Not Pres-ent	5.18	52.72
Rectangular Patch with Reduced Ground	2.91	-8.53	Not Pres-ent	Not Pres-ent	3.77	94.16
Lotus Patch with Reduced Ground	2.95	-21.41	2.14-3.14	33.89	3.09	93
Lotus Patch with Compressed Ground	2.88	-29.43	2.06-3.12	36.80	3.02	94
Lotus Patch with Compressed Ground and SRR Quadruplet	2.87	-28.36	2.06-3.07	35.17	3.22	92
Lotus Patch with compressed ground and relocated SRR quadruplet and their orientations	2.04, 2.27, 2.90	-36.45, -28.64, -18.65	1.61-3.24	57.19	1.15, 1.04, 3.56	81, 82, 92

C. Variation of Ground (Full to Monopole GND)

To improve the antenna radiation efficiency, wideband performance, and antenna gain changes in the ground plane have been observed. Initially, the full ground (44mm × 40mm) surface beneath the lotus-shaped patch has no significant results in terms of antenna resultant parameters. Therefore, antenna ground length is reduced to 7.5 mm towards the feed line. This makes the antenna monopole.

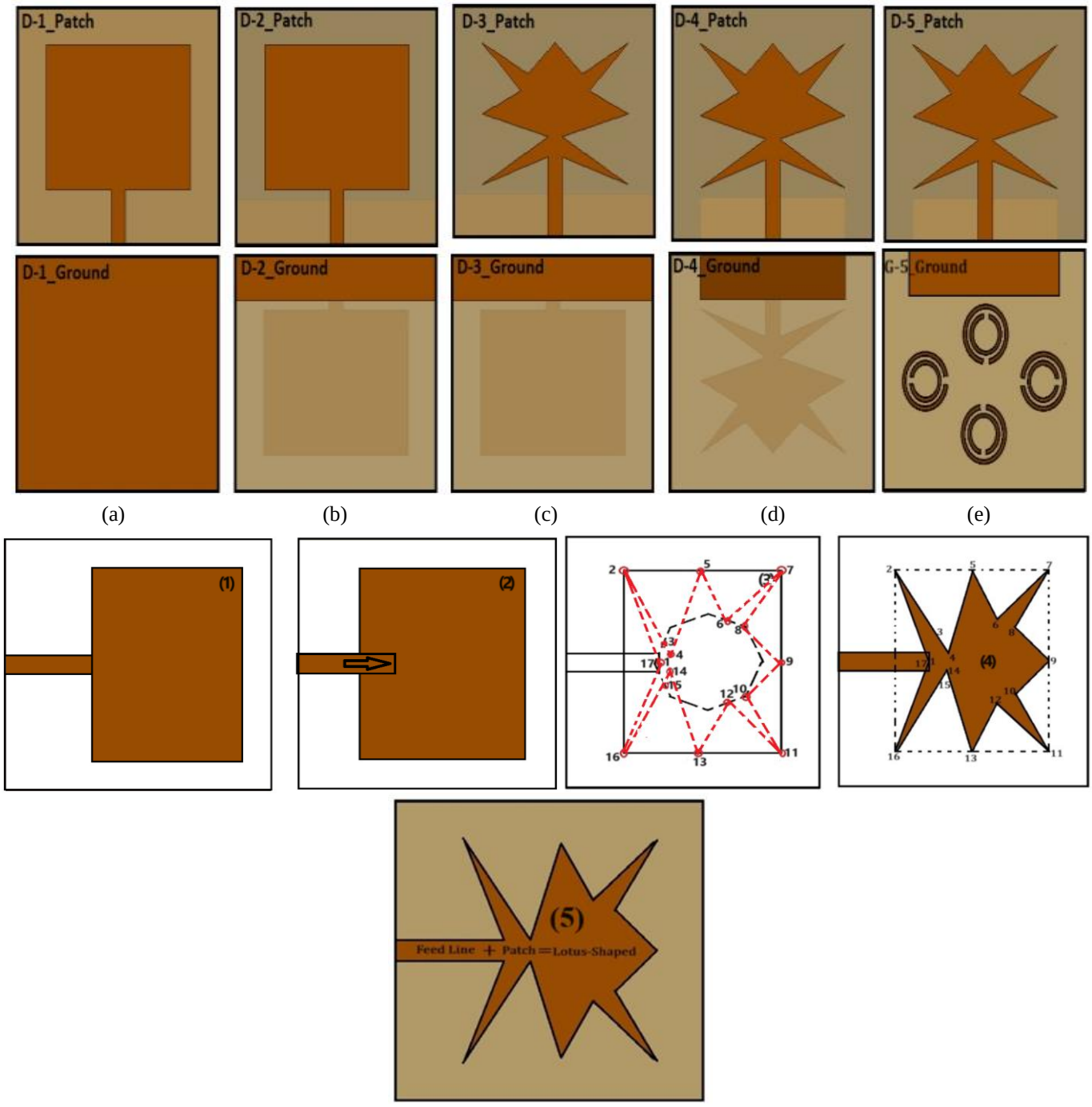

Fig. 2. Design Development from Rectangular Patch to Lotus-Shaped Monopole Antenna: (a) Design-1, (b) Design-2, (c) Design-3, (d) Design-4, (e) Design-5 (f) Operations involved in the generation of seven arm lotus-shaped patch geometry

This will result in improved antenna radiation efficiency and decade FBW. This offers a reduction in the surface currents. The further compressed ground width (33mm) symmetrically around the feed results in approximately 3% wideband performance with a minor decrease in the antenna gain. Further, the gain value is improved by parasitic loading with four SRR quadruplets on the ground surface. All four SRRs are placed at the position of the minimum surface current positions in patch arms with all their rings cut orientations in phase (0°). This will result in an improved gain value of 3.22 dBi. Furthermore, the -10 dB fractional bandwidth is increased by relocating the SRRs positions on the ground surface across the Lotus arms and by keeping SRR rings orientation out of phase (180°). This relocation of SRRs and their ring orientation 180° widened the -10 dB BW to 57.19% (1.61GHz to 3.24 GHz). The effect of modified

ground is analyzed and summarized in Table 4 and the family of variations in ground modifications are illustrated in Fig. 3.

TABLE 4
GROUND MODIFICATIONS

Ground shape modification	Reson. Freq. f_r (GHz)	Ref Coeff., S_{11}(dB)	Band (GHz)	-10dB FBW (%)	Gain (dBi)	Rad. Eff. (%)
With Full Ground Without SRR	2.44	-2.45	Not exist	Not exist	-5.97	7
With reduced Ground without SRR	2.95	-21.41	2.14-3.14	33.89	3.09	93
Compressed Ground Without SRR	2.88	-29.43	2.06-3.12	36.80	3.02	94
Compressed Ground with SRR Quadruplet	2.87	-28.36	2.06-3.07	35.17	3.22	92
Lotus Patch with compressed ground and relocated SRR quadruplet and their orientations	2.04, 2.27, 2.90	-36.45, -28.64, -18.65	1.61-3.24	57.19	1.15, 1.04, 3.56	81, 82, 92

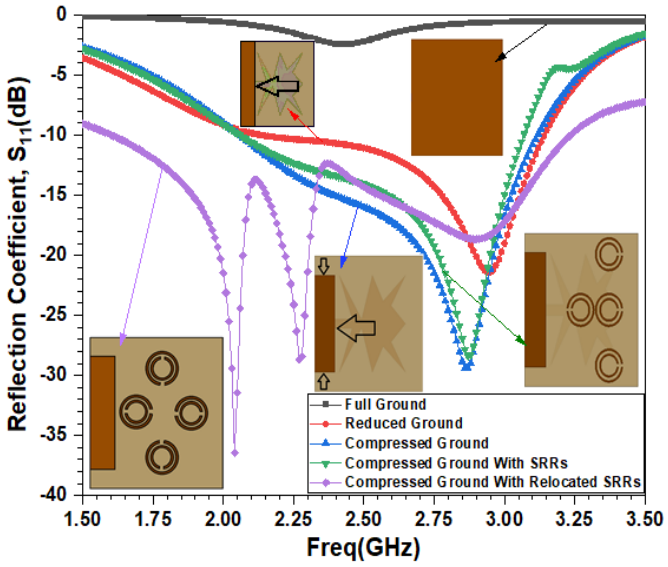

Fig. 3. Effect of Ground Modifications

D. Effect of Introduced SRR: (Without SRR and with SRR)

The lotus-shaped monopole antenna is practically loaded with four SRRs called parasitic loading of SRR-Quadruplets. The effect before loading without SRR-quadruplets and after loading with SRR-quadruplets has been analyzed. Finally, the positions and orientations are rearranged on the bottom ground surface. The step-by-step variations of these parasitic loading effects are showcased in Table V and their reflection coefficient comparisons are depicted in Fig. 4. It has been observed that the SRR loading results in Gain enhancement on the cost of the slight reduction in their radiation efficiency and decade FBW.

TABLE 5
EFFECT OF PARASITIC LOADING OF SRR QUADRUPLETS

Effect of Parasitic Loading of SRR Quad-ruplets	Reson. Freq., f_r(GHz)	Ref. Coeff., S_{11}(dB)	Band (GHz)	-10dB FBW (%)	Gain (dBi)	Rad. Eff. (%)
Without SRR	2.88	-29.43	2.06-3.12	36.80	3.02	94
With SRR orientation 0°	2.87	-28.36	2.06-3.07	35.17	3.22	92
Effect of SRRs orientation 180° and placement location change	2.04, 2.27, 2.90	-36.45, -28.64, -18.65	1.61-3.24	57.19	1.15, 1.04, 3.56	81, 82, 92

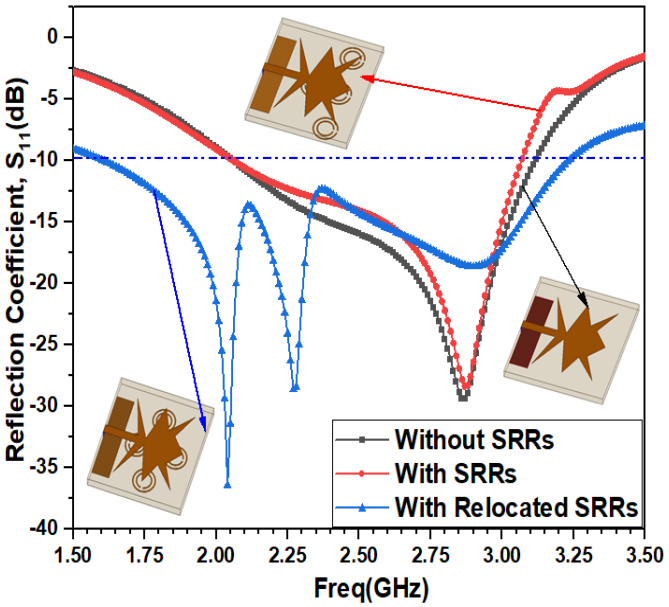

Fig. 4. Effect of Introduced SRR

III. RESULTS AND DISCUSSION

The antenna is fabricated on the FR4 substrate of size 44mm×40mm by film making, photolithography, UV exposure, and chemical etching process. The front and rear views of the fabricated antenna are represented in Fig. 5(a-b). The SRRs quadruplet's positions and orientations of their rings are again further readjusted to enhance the bandwidth and this adjustment also allows the antenna to be tuned at three resonating frequencies. The newly fabricated prototypes' front and rear views are displayed in Fig. 5(c-d). The reflection coefficients of the two prototyped antennas are measured on a vector network analyzer (VNA) Agilent N5247A. The simulated and measured reflection coefficient results are plotted on the same scale of frequency as shown in Fig. 5(e). The comparison results of both the prototype antenna models are arranged in Table VI. It is observed that

the measured antenna reflection coefficient drops the lowest value -44.30 dB at a frequency of 2.79 GHz while in simulated the lowest value of reflection coefficient is observed at 2.87 GHz. The measured wideband lower than -10 dB is observed for a frequency range from 1.91 GHz to 3.0 GHz. The measured FBW is 39.06% as compared to the simulated FBW of 35.17%. Therefore, the measured fabricated antenna holds a good agreement with the designed simulated antenna. The new prototyped antenna model measured reflection coefficient drops the lowest value -34.98 dB, -28.01 dB, and -19.91 dB at three resonating frequencies 2.02 GHz, 2.31GHz, and 2.84 GHz respectively. In simulated the lowest value of reflection coefficient are observed -36.45 dB, -28.64 dB, and -18.65 dB at three resonating frequencies 2.04 GHz, 2.27 GHz, and 2.90 GHz. The measured wideband -10dB BW is observed for a frequency range from 1.52 GHz to 3.13 GHz. The measured FBW is 56.49% as compared to the simulated FBW of 57.19%. It is concluded from the observations that the orientation of SRR rings and their placement in the right locations results in an enhancement in antenna bandwidth.

The radiation pattern and gain of the antenna are observed in the 18 GHz anechoic Chamber as displayed in Fig. 6(a). The simulated and measured E-plane and H-plane gain radiation patterns at the resonance frequency of 2.87 GHz for antenna without SRR loading, with SRR-quadruplets loading are plotted in the polar plots of Fig. 6(b-c) and these are found in approximations. The relocated SRRs-quadruplet loading and 180° orientation of SRRs rings simulated and measured gain radiation patterns in E-plane and H-plane are depicted in Fig. 6(d(i)–d(iii)) at three resonating frequencies 2.04 GHz, 2.27 GHz, and 2.90 GHz respectively. The 3D-radiation patterns of the antenna without SRR and With SRR-quadruplets loading are shown in Fig. 7(a-c). These are omnidirectional in the E-plane and Fig. of Eight-like shape in the H-plane.

TABLE 4
PROPOSED ANTENNA RESULTANT PARAMETERS

Results Validation	Reson. Freq. f_r GHz)	Ref Coeff., S_{11}(dB)	Band (GHz)	-10dB FBW (%)	Gain (dBi)	Rad. Eff. (%)
Simulated	2.87	-28.36	2.06-3.07	35.17	3.24	92
Measured	2.79	-43.40	1.91-3.0	39.06	4.07	-----
SRRs orientation (180°) and placement location change (Simulated)	2.04, 2.27, 2.90	-36.45, -28.64, -18.65	1.61-3.24	57.19	1.15, 1.04, 3.56	81, 82, 92
SRRs orientation (180°) and placement location change (Measured)	2.02, 2.31, 2.84	-34.98, -28.01, -19.91	1.52-3.13	56.49	3.51, 3.42, 3.43	-----

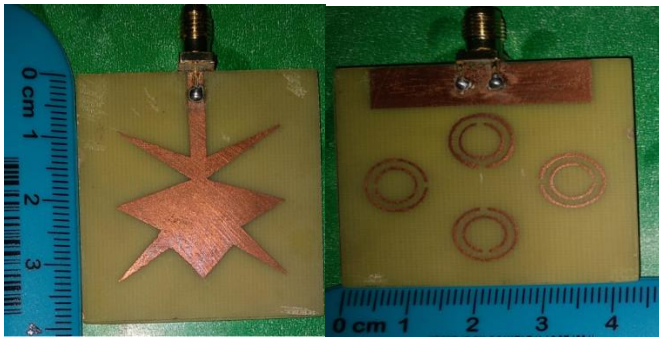

(a) (b)

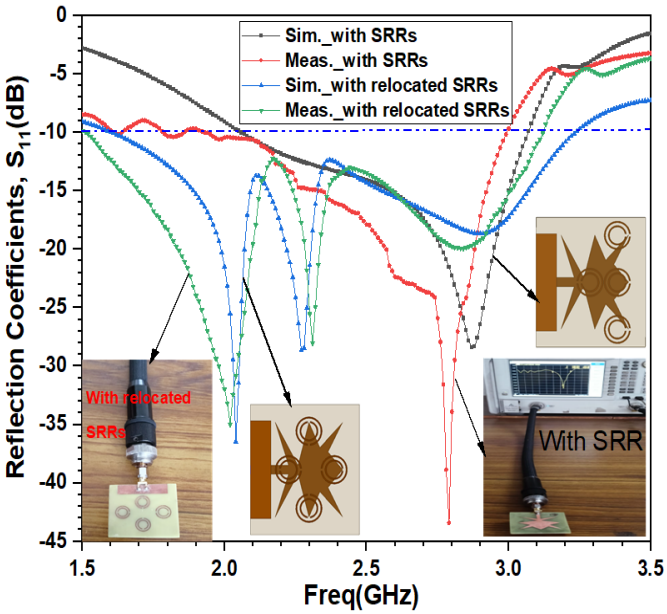

(c)

Fig. 5. Fabricated antenna Prototype Model: (a) Front View, (b) Rear View, and (c) Reflection Coefficients (Sim. vs Meas.)

With 0° orientations of SRR-quadruplet loading the measured peak gain at resonance frequency is 4.07dBi while the simulated gain is 3.22 dBi. The simulated and measured gains are plotted in the same Fig. for the frequency sweep 1.5 GHz to 3.5 GHz. The measured gain value is higher than the simulated gain value over the entire band of interest. The measured antenna a gain at the resonance frequency is 4.07 dBi at the resonance frequency of 2.85 GHz as illustrated in Fig. 8. With 180° orientations and relocation of SRR-quadruplet loading the measured peak gain at resonance frequency is 4.70 dBi while the simulated gain is 3.22 dBi. The difference between simulated and measurement gains is due to the soldering error of 50 Ω connector, and dimensional margin error of fabricated and simulated dimensions as the main reason is due to different parasitic effects in fabrication and simulated antenna design due to the parasitically placed SRRs quadruplets. After parasitic loading with SRR-quadruplets, the efficiency remains constant at 92% while the antenna peak gain is enhanced to 3.60 dBi. The simulated peak gain and efficiencies are plotted on double verticle axes to the same horizontal frequency axis as displayed in Fig. 9.

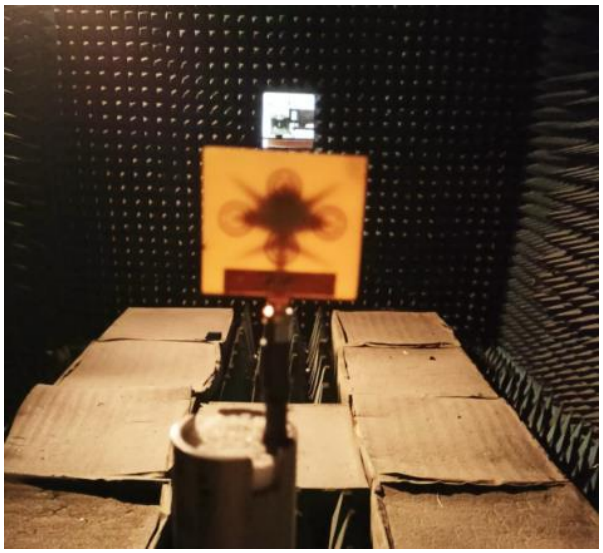

(a)

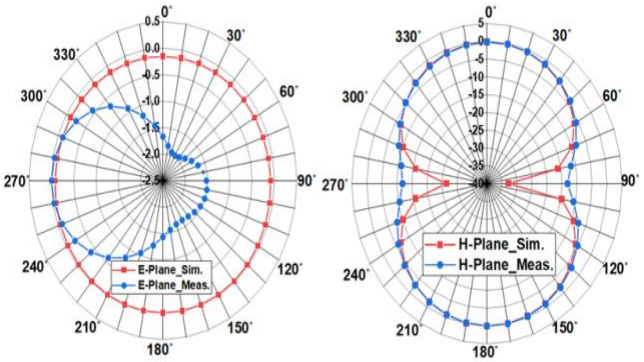

(b)

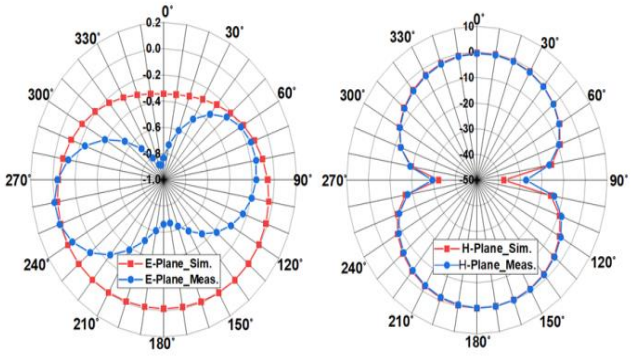

(c)

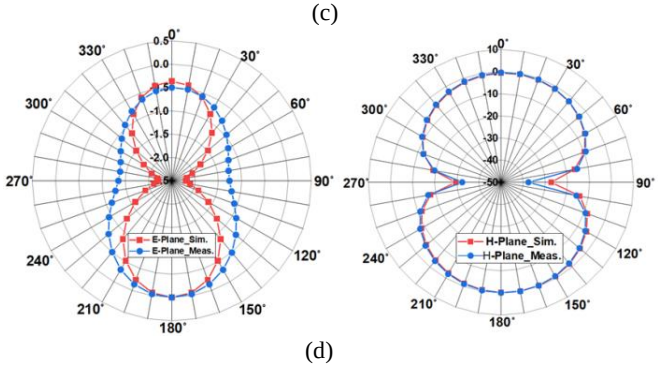

(d)

Fig. 6. Radiation Patterns: (a) Anechoic Chamber Measurements, E-Plane and H-plane radiation patterns for SRRs at (b) 2.04 GHz, (c) 2.27 GHz, and (d) 2.90 GHz

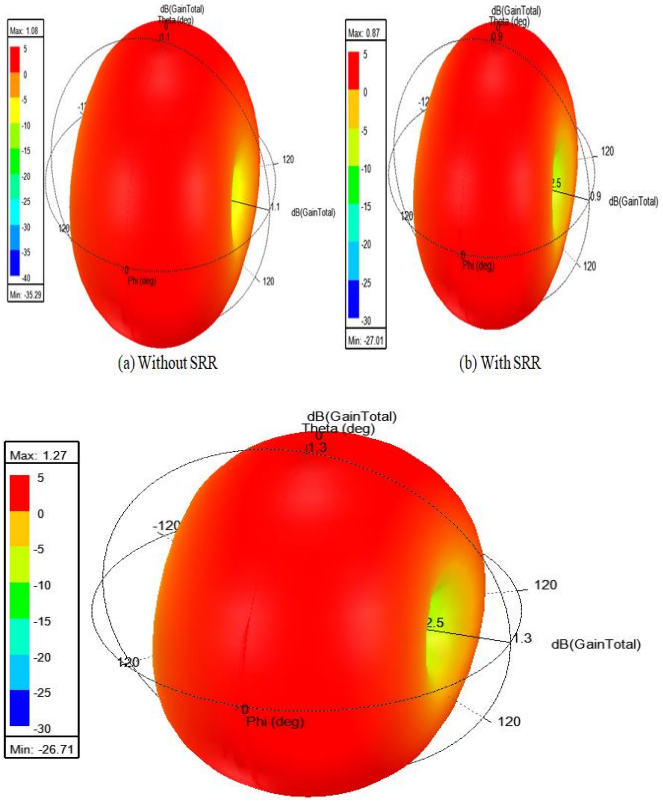

Fig. 7. 3D-Radiation Gain Pattern without and with SRR-Quadruplet

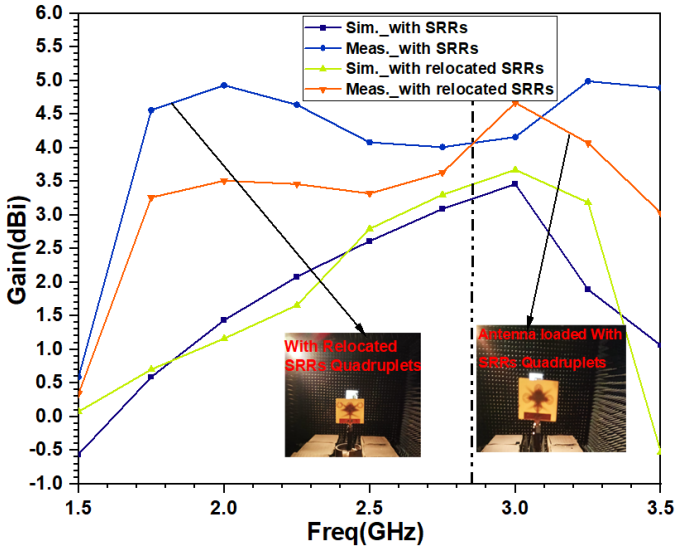

Fig. 8. Antenna Gains (Sim. vs Meas.)

A. Electrical Equivalent of SRR

All four SRR units are evaluated and designed using the standard equations at a designed frequency of 2.85 GHz [31, 32]. Each of the SRRs individually behaves like an LC tank circuit with an inductance value of 17.5455 nH and a capacitance value of 0.18 pF. The equivalent circuit of the single-unit SRR is represented in Fig. 10.

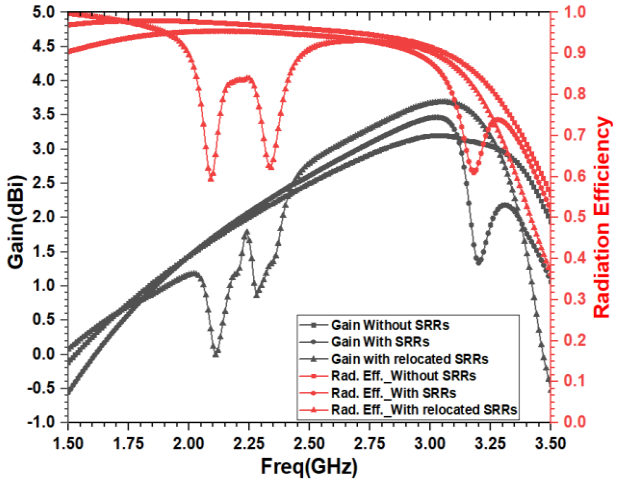

Fig. 9. Gain and Efficiency

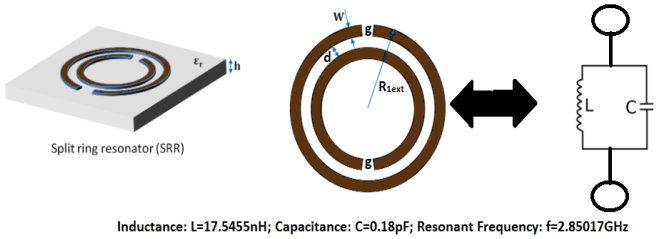

Fig. 10. Electrical Equivalent of SRR

B. Electrical Equivalent Circuit of Proposed Antenna

The RLC electrical equivalent circuit of the lotus-shaped antenna whose ground is loaded with four in-phase (0°) SRRs ring orientations is initially derived from the reflection coefficient S_{11}, and impedance Z_{11} plots of HFSS software by simple resonance theory and circuit network analysis using series parallel resonance circuits.

The S_{11} plot consists of two stop bands and one passband with a resonance frequency of 2.87 GHz. The first stop band and passband show the low real parts and are therefore represented by a series RLC resonance circuit in a parallel branch while the third stop band shows a high real impedance value that shows the parallel resonance in the series arm. The manually evaluated RLC values are displayed in Fig. 11(a). Finally, the circuit is tuned using ADS software as displayed in Fig. 11(b). The reflection coefficient plots of the HFSS software and ADS software are plotted in Fig. 12 and they are found in closeness. This validated the RLC circuits of the proposed Lotus-shaped monopole antenna [16, 2, 4, 3, 14, 33, 15].

Similarly, the RLC electrical equivalent circuit of the lotus-shaped antenna whose ground is loaded with four out-of-phase (180°) SRRs ring orientations is also derived from the reflection coefficient S_{11}, and impedance Z_{11} plots of HFSS software by resonance theory and circuit network analysis using series parallel resonance circuits [14]. The S_{11} plot consists of two stop bands and one passband with triple resonance frequencies at 2.04 GHz, 2.27 GHz, and 2.90 GHz. The first stop band and passband show the low real parts i.e. 9.44 Ω and are therefore represented by a series RLC resonance circuit in a parallel branch while the second stopband shows a high impedance magnitude value i.e. 103.946 Ω that shows the parallel resonance in the series arm. The passband of the reflection coefficient consists of three resonance frequencies with impedance magnitudes values 48.75 Ω, 51.10 Ω, and 78.34 Ω respectively. The first two resonance frequencies in the -10 dB FBW correspond to the series RLC circuits as per the low impedance rule while the third resonating frequency is corresponding to the parallel resonance. The series combinations of all these three resonating circuits form the complete passband of the proposed lotus-shaped antenna. The manually evaluated RLC values are displayed in Fig. 11(c). Finally, the circuit is tuned using ADS software as displayed in Fig. 11(d). The reflection coefficient plots of the HFSS software and ADS software are plotted in Fig. 12 and they are found in closeness. This validated the RLC circuits of the proposed Lotus-shaped monopole antenna [2, 3, 4, 14, 28, 33].

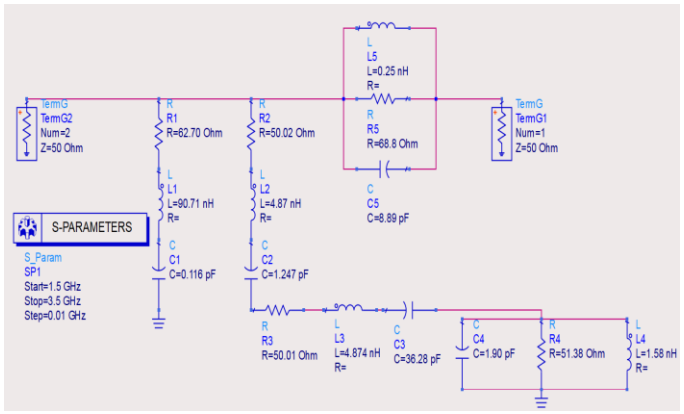

(a)

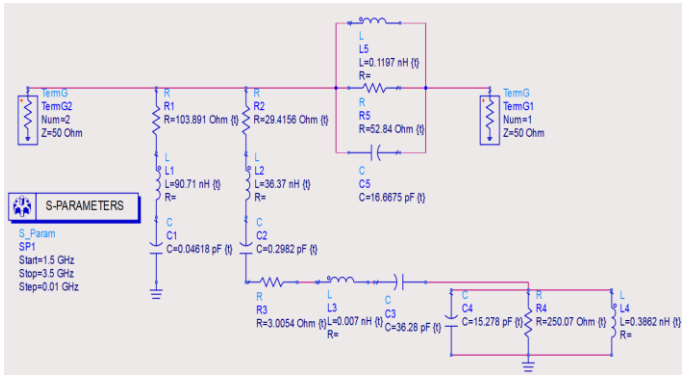

(b)

Fig. 11. RLC Electrical Equivalent Circuit of Proposed Antenna: (a) ADS (after tuning with SRR Rings orientation=180°), (b) ADS circuit after tuning for relocated SRR (with SRR Rings orientation=180°)

C. Current Density Distributions

The magnitude of current density distributions at the three resonance tunning frequencies 2.04 GHz, 2.27 GHz, and 2.90 GHz are illustrated in the Fig. 13(a-c), respectively. At the resonant frequencies 2.04 GHz, 2.27 GHz, the most of the current is confined in feed line and top three lotus arms as shown in Fig. 13(a) and Fig. 13(b). In these cases, only one SRR (upper) has the maximum current while the other three

SRRs are having lowest current. At 2.27 GHz the current in the lotus patch arm is higher as compared to the 2.04 GHz tunning frequency. On the other hand, at third resonant tuning frequency 2.90 GHz the two SRRs has the maximum currents while the rest two SRRs has the lowest current magnitudes. These will consequently improve the current density magnitudes in the whole lotus arms patch as shown in Fig. 13(c).

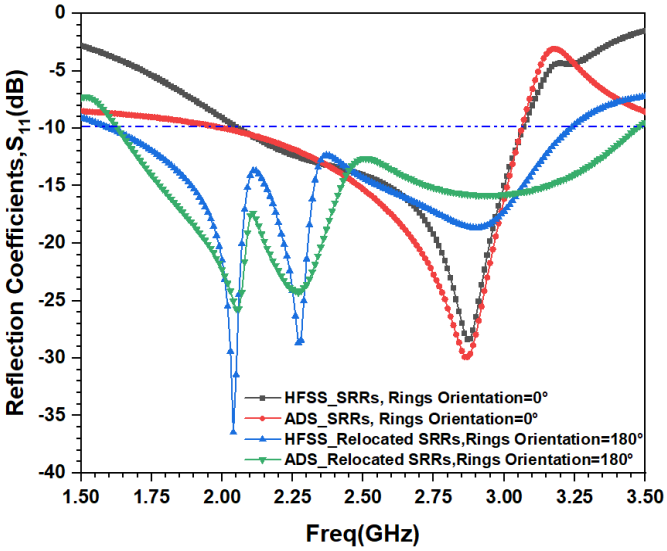

Fig. 12. RLC Electrical Equivalent Circuit Validation of Proposed Antenna: (a) HFSS Manual, (b) ADS

D. Comparison with the Similar Existing Literature Antennas

The proposed antenna is compared with the similar recently published antennas in Table 7. It is observed from the comparison table that most of the antennas were designed with the use of cut, slots, CSRR, and SRR, and some of the antennas were designed with the use of SRR/CSRR along with fractal to modify the radiation and reflection characteristics of the antenna parameters. The proposed antenna is designed with a special-shaped cut (as displayed in Fig. 2(f)) from the rectangular patch to make a symmetrical lotus-shaped patch and parasitically loaded with the SRR-Quadruplets to maintain the deuced value of gain due to the fractal cut. The antenna is fabricated on the FR-4 substrate instead of the RT Duroid 5880 low-loss substrate. This makes the proposed antenna economical and low profile. The antenna shows a good impedance match at the resonance frequency of 2.85 GHz with an excellent reflection coefficient value. The antenna is best suitable for wideband applications within the decade bandwidth from 2.06 GHz to 3.07 GHz. This wideband is mostly suitable for weather RADAR, Satellite digital audio radio services (SDARs), and Wireless Communication Services (WCS). The antenna attains a good gain of 3.22dBi and a radiation efficiency of 92%. The structure of the antenna is simple as compared to others as the radiating patch does not contain any slot. Therefore, the fabrication of this antenna is not tedious.

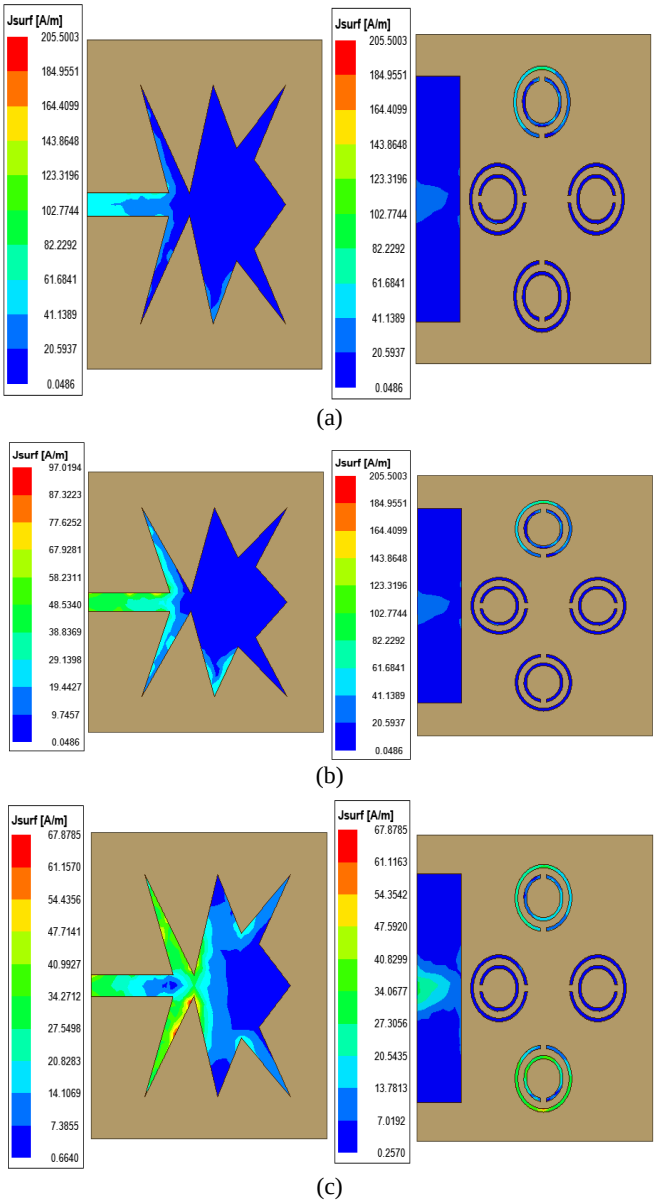

Fig.13 Magnitude of Current density distributions at: (a) 2.04 GHz, (b) 2.27 GHz, and (c) 2.90 GHz

IV. CONCLUSION

The novel techniques used in the rectangular patch increase the overall electrical length of the patch and make the antenna flexible to be used for other applications too. A new type of modified rectangular patch antenna with seven arms lotus-shaped parasitic SRR loading has been analysed, fabricated, and tested. When the antenna is loaded with SRR-quadruplets at the minimum current positions of the lotus arms with 0° orientations, then the measured gain at the designed frequency was 4.07 dBi and the reflection coefficient decade fractional bandwidth (FBW) was 39.07% (2.06 GHz - 3.07 GHz) which results in wideband performance and covers the applications like IoT, WCDMA (2110-2170 MHz), ISM (2.4-2.5 GHz), 3G (2.1 GHz), 2.4 GHz band used by more than 300 consumer devices, including domestic Microwave ovens, WLAN, cordless phones, cellular PCS and wireless networks (Bluetooth and Wi-Fi), satellite radio (2.3 GHz), 4G-LTE

TABLE 7
COMPARISON OF SIMILAR EXISTING ANTENNAS

Ref.	Substrate /Cost	Design freq., f_o (GHz) and (Feed type)	Antenna size (mm^3)	Res. Freq., (*fr* GHz)	Band (GHz)	FBW (%)	Gain (dBi) and Rad. Eff. (%)	Cut/slot/ SRR/CSRR used	Applications
[12]	FR-4 ε_r = 4.4 Low cost	10.0 (CPW)	14× 16× 1.6	2.5, 3.58 5.73, 8.025 12.45 16, 18.43	1.836-4.319 4.92-8.89 11.92-12.86 15.3-19.44	80.68 57.49 7.58 23.83	3.9	Leaf-shaped, Koch fractal, SRR used	WLAN, RFID, Satellite, MW relay, HyperLAN, RADAR
[13]	FR-4 ε_r =4.4 Low cost	3.8 (Edge)	30× 30× 1.6	2.9,5.0, 9.0	2.94-12.0	44.8, 40, 78	5.57, 5.37, 6.75/ 85.54%	C-shaped slot and CSRR slot	Wi-MAX, WLAN
[14]	FR-4 ε_r =4.4 Low Cost	2.45 (Edge)	66.4× 66.4× 1.6	2.5	1.81-3.0	49	7.16/ 92.85%	Fan-Shaped; SRR triplets	Wi-MAX, Wi-Fi, GSM, public safety band, Bluetooth, ISM band, 3G, 4G LTE, WCDMA, PCS applications.
[17]	Rogers 5880 ε_r =2.2 Costly	2.4 (Off-Set)	28× 21× 1.6	2.4	2.36-2.5	5.80	2.09/ 98%	L-shaped, no SRR	ISM bands and IoT applications, fourth generation (4G) WCS
[19]	Roger 5880 ε_r =2.2 costly	3.01 (Transformer)	35× 35× 1.57	18.2, 37.82	3.2-30	174.60	5.9/ 92.7%	S-Shaped, No SRR	WIMAX, UWB, WLAN, ISM
[20]	FR-4 ε_r =4.4 Low cost	2.1 (CPW)	60× 60× 1.6	With U-Slot 2.4 4.6,5.8, 6.2 9.2 With L-Slot 2.1 3.7 5.3	With U-Slot (2.1-2.8) (4.0-7.5) & (8.2-9.8) With L-Slot (1.9-2.3) (3.4-4.0) (4.8-5.8)	With U-Slot 28.57, 60.86, 17.77 With L-Slot 19.04, 16.21, 18.86	4.2	Circular disk, no SRR	WLAN WiMAX HiperLAN
[22]	FR-4 ε_r =4.4 Low cost	2.89 (Edge)	30× 20× 1.6	2.6, 3.4	2.3-3.4	40.13	4.07, 3.90 / 96.2%	Rectangular Patch, SRR used	Wi-MAX, WLAN, Bluetooth, LTE
[23]	Rogers 5880 ε_r =2.2 Costly	3.0 (Edge)	20× 24× 1.5	7.4, 15, 22.3	3-27.5	160.66	6.3 /93%	Human Skulled-shaped,no SRR	LAN/ Wi-Fi/ Wi-MAX/ UWB
[25]	FR-4 Low-cost	9.13 (CPW)	31× 30×1.8	-----	3.8 - 14.4	116	5.9	Lotus-shaped/ No SRR	C, X, and partially Ku bands
[33]	FR-4 Low-cost	2.45 (Edge)	66.4× 66.4× 1.6	2.02, 2.29, 2.57	1.63-2.91	52.65	3.89/ 94.09%	CSRR-slotted, Tri-arms, CSRR used	ISM and PCS Communications
This Work	FR-4 Low-cost	2.85 (Inset)	44× 40× 1.6	2.04, 2.27, 2.90	1.61-3.24	57.19	1.15/81%, 1.04/82%, 3.56/92%	Lotus-shaped with seven arms, SRR used	Satellite Radio, WPC, SDARs, and Weather Radar

(2.17–2.32 GHz), weather radar (2.7-2.9 GHz), 5G n41(2.5 GHz), and WCS (2.305-2.365 GHz, 2.32-2.345 GHz), 5G bands n1(2.1 GHz), n7(2.6 GHz), n40(2.3 GHz), n41(2.5 GHz), n48(3.5 GHz), n30(2.3 GHz), n34(2.1 GHz), n95(2.1 GHz), n97(2.3 GHz). Further, a modified antenna is designed, refabricated, and measured by relocating the SRRs-quadruplet and arrangments of their ring cut orientations at 180° on the ground plane along with the unchanged compressed ground. This offers triple-tuned wideband from 1.61 GHz to 3.24 GHz and resonates at frequencies 2.04 GHz, 2.27 GHz, and 2.90 GHz with FBW 57.19%. The modified structure additionally covers applications like cellular PCS (1.90-1.99 GHz), GSM (1800 MHz), 5G bands n2(1.9 GHz), n3(1.8 GHz), n25(1.9 GHz), n39(1.9 GHz), n70(2.0 GHz), n80(1.8 GHz), n86(1.7 GHz), n98(1.9 GHz). The simulated and measured results are found to be agreement with acceptable deviation in the resonance frequency, fractional bandwidth, antenna gain, and radiation patterns. These daviations are because of the fabrication tolerances, and soldering of the SMA connector location error, and measurement errors. The antenna reflection coefficient is double-validated using VNA and ADS software.

In the future, the gain of the antenna could be enhanced by a great amount by using frequency selective surface, resistive interference surface, artificial magnetic conductor, or metamaterial SRR surface beneath the antenna ground layer at the suitable optimized location. Therefore, it is concluded that frequency reconfigurability could be achieved by the increase in the number of iterations. This will add an extra possibility to make the antenna multiband.

ACKNOWLEDGEMENT

The authors are grateful to Hon'ble Vice-Chancellor, Gurukula Kangri (Deemed to be University), Haridwar, India for providing software and hardware support for conducting the project.

REFERENCES

[1] A. Varshney and V. Sharma, "A Comparative Study of Microwave Rectangular Waveguide-To-Microstrip Line Transition for Millimeter Wave, Wireless Communications and Radar Applications", in *Microwave Review*, vol. 2, no. 26, pp. 26-37, 2020, ISSN 14505835

[1] A. Varshney and V. Sharma, "Aerodynamic Slotted SIW-to-MS Line Transition Using Mitered End Taper For Satellite and Radar Communications", in *World Journal of Engineering*, 2023, DOI: 10.1108/WJE-08-2022-0330

[2] A. Varshney, V. Sharma, I. Elfergani, S. R. Kannan, R. Udaiyakumar, C. Zebiri and R. Abd-Alhameed, "An Economic Low-profile Elliptical Microstrip Antenna-to-RWG Transition for Microwave Laboratory and X-Band Applications", in *Research Square Platform LLC*, 2023, DOI: 10.21203/rs.3.rs-2357185/v1

[3] A. Varshney, V. Sharma and R. Kumar, "Microstrip Interconnect Design and Modeling Using Reverse Approach To Obtain An Efficient Wideband MS Line-to-RWG Hybrid Transition", in *Printed Antennas: Design and Challenges*, vol. 67, 2022, DOI: 10.1201/9781003347057-5

[4] A. Varshney, V. Sharma, C. Nayak, A. K. Goyal and Y. Massoud, "A Low-Loss Impedance Transformer-Less Fish-Tail-Shaped MS-to-WG Transition for K-/Ka-/Q-/U-Band Applications", in *Electronics*, vol. 12, no. 3, p. 670, 2023, DOI: 10.3390/electronics12030670

[5] K. Mahendran and R. Gayathri, "Performance Improved Triangular Multi-Band Antenna Using Reactive Impedance Substrate and Frequency Selective Surface", in *Information Technology in Industry*, vol. 9, no. 1, pp. 486-492, 2021, DOI: 10.17762/itii.v9i1.159

[6] A. J. A Al-Gburi, I. B. M. Ibrahim, M. Y. Zeain, and Z. Zakaria, "Compact Size and High Gain Of CPW-Fed UWB Strawberry Artistic Shaped Printed Monopole Antennas Using FSS Single Layer Reflector", in *IEEE Access*, vol. 8, pp. 92697-92707, 2020, DOI: 10.1109/ACCESS.2020.2995069

[7] F. A. Tahir, T. Arshad, S. Ullah and J. A. Flint, "A Novel FSS for Gain Enhancement of Printed Antennas in UWB Frequency Spectrum", in *Microwave and Optical Technology Letters*, vol. 59, no. 10, pp. 2698-2704, 2017, DOI: 10.1002/mop.30789

[8] F. M. Monavar and N. Komjani, "Bandwidth Enhancement of Microstrip Patch Antenna Using Jerusalem Cross-Shaped Frequency Selective Surfaces by Invasive Weed Optimization Approach", in *Progress in Electromagnetics Research*, vol. 121, pp. 103-120, 2011, DOI:10.2528/PIER11051305

[9] Y. Yuan, X. Xi, Y. Zhao, "Compact UWB FSS Reflector for Antenna Gain Enhancement, in *IET Microwaves, Antennas & Propagation*", vol. 13, no.10, pp. 1749-1755, 2019, DOI: 10.1049/iet-map.2019.0083

[10] R. A. Abdulhasan, R. Alias, K. N. Ramli, F. C. Seman, R. A. Abd-Alhameed, "High Gain CPW-Fed UWB Planar Monopole Antenna-Based Compact Uniplanar Frequency Selective Surface for Microwave Imaging", in *International Journal of RF and Microwave Computer Aided Engineering*, vol. 29, no. 8, e21757, 2019, DOI: 10.1002/mmce.21757

[11] C. Elavarasi and T. Shanmuganantham, "Multiband SRR Loaded Leaf-Shaped Koch Fractal with a Modified CPW-Fed Antenna", in *International Journal of Electronics Letters*, vol. 6, no. 2, pp. 137-145, 2018, DOI: 10.1080/21681724.2017.1329942

[12] N. Sharma, S. S. Bhatia, V. Sharma and J. S. Sivia, "An Octagonal Shaped Monopole Antenna for UWB Applications with Band Notch Characteristics", in *Wireless Personal Communications*, vol. 111, pp. 1977-1997, 2020, DOI: 10.21608/iceeng.2014.30386

[13] A. Varshney, N. Cholake and V. Sharma, "Low-Cost ELC-UWB Fan-Shaped Antenna Using Parasitic SRR Triplet for ISM Band and PCS Applications", in *International Journal of Electronics Letters*, vol. 10, no. 4, pp. 391-402, 2022, DOI: 10.1080/21681724.2021.1966655

[14] Wireless Communications Service (WCS), Federal Communications Commission, 2017-03-08, Retrieved 2018-04-08, Accessed on 30-05-2023.

[15] A. Varshney, V. Sharma, I. Elfergani, C. Zebiri, Z. Vujicic and J. Rodriguez, "An Inline V-Band WR-15 Transition Using Antipodal Dipole Antenna as RF Energy Launcher @ 60 GHz for Satellite Applications", in *Electronics*, vol. 11, no. 23, 3860, 2022, DOI: 10.3390/electronics11233860

[16] M. F. Zambak, S. S. Al-Bawri, M. Jusoh, A. H. Rambe, H. Vettikalladi, A. M. Albishi and M. Himdi, "Compact 2.4 GHz L-Shaped Microstrip Patch Antenna for ISM-Band Internet of Things (IoT) Applications", in *Electronics*, vol. 12, no. 9, p. 2149, 2023, DOI: 10.3390/electronics12092149

[17] A. Ghaffar, X. J. Li, W. A. Awan, S. Iffat Naqvi, N. Hussain, B. C. Seet and E. Limiti, "Design and Realization of a Frequency Reconfigurable Multimode Antenna For ISM, 5G-sub-6-GHz, and S-band Applications", in *Applied Sciences*, vol. 11, no. 4, p. 1635, 2021, DOI: 10.3390/app11041635

[18] S. Ullah, C. Ruan, M.S. Sadiq, T.U. Haq, A.K. Fahad and W. He, "Super Wide Band, Defected Ground Structure (DGS), and Stepped Meander Line Antenna for WLAN/ISM/Wimax/UWB and Other Wireless Communication Applications", in *Sensors*, vol. 20, no. 6, p. 1735, 2020, DOI: 10.3390/s20061735

[19] Z. Mansouri, F. B. Zarrabi and A. S. Arezoomand, "Multi Notch-Band CPW-Fed Circular-Disk UWB Antenna Using Underground Filter", in *International Journal of Electronics Letters*, vol. 6, no. 2, pp. 204-213, 2018, DOI: 10.1080/21681724.2017.1335786

[20] D. Fonseca, F. Pereira and U. R. Vitor, "Study of Patch Antennas with Koch Curve Form Slots", in *Journal of Microwaves, Optoelectronics and Electromagnetic Applications*, vol. 18, pp. 399-407, 2019, DOI: 10.1590/2179-10742019v18i31672

[21] M. Sharma, N. Mishra and R. K. Chaudhary, "SRR Based Compact Wideband Metamaterial Inspired Antenna for WiMAX (2.5-2.7)/WLAN (2.4-2.48)/Bluetooth (2.4-2.48)/LTE (2.3-2.4) Applications", in *Progress in Electromagnetics Research Letters*, vol. 80, pp. 109-116, 2018, DOI: 10.2528/PIERL18100802

[22] M. A. Rahman, M. S. J. Singh, M. D. Samsuzzaman and M. T. Islam, "A Compact Skull-Shaped Defected Ground Super Wideband Microstrip Monopole Antenna for Short-Distance Wireless Communication", in *International Journal of*

Communication Systems, vol. 33, no. 14, e4527, 2020, DOI: 10.1002/dac.4527

[23] A. Varshney, T. M. Neebha, V. Sharma, J. G. Jency and A. D. Andrushia, "Dodecagon-Shaped Frequency Reconfigurable Antenna Practically Loaded With 3-Delta Structures for ISM Band and Wireless Applications**"**, in *IETE Journal of Research*, pp. 1-13, 2022, DOI: 10.1080/03772063.2022.2034536

[24] A. Antony and B. Dasgupta, "Design and Analysis of a Frequency Selective Surface Loaded Bioinspired Antenna in Frequency and Time Domains", in *Progress in Electromagnetics Research M*, vol. 116, 2023, DOI: 10.2528/PIERM23010302

[25] D. Sudarshan, Y. K. Choukiker, S. K. Behera and O. K. Kennedy, "Compact Lotus Shape Planar Microstrip Patch Antenna for UWB Application", *IEEE Applied Electromagnetics Conference*, 2013.

[26] M. Samsuzzaman, M. Z. Mahmud, M. T. Islam, M. M. Ali and M. T. Islam, "Compact Lotus Shape Dual Band Patch Antenna For Bluetooth and Ultra Wideband Applications", in *Microwave and Optical Technology Letters*, vol. 59, no. 7, pp. 1590-1597, 2017, DOI: 10.1002/mop.30589

[27] A. Varshney, V. Sharma and A. K. Sharma, "RLC-Equivalent Circuit Based Stub Loaded 2x2 MIMO Antenna for Wireless Applications", in *Microwave Review*, vol. 29, no. 1, 2023, ISSN 2406-1050

[28] K. Chang, *RF and Microwave Wireless Systems*, John Wiley & sons, 2004, ISBN: 978-0-471-46387-0

[29] C. A. Balanis, *Antenna theory: Analysis and design*, John Wiley & Sons, 2016, ISBN: 978-1-118-64206-1

[30] V. Sharma, S. S. Pattnaik, T. Garg and S. Devi, "A Microstrip Metamaterial Split Ring Resonator", in *International Journal of Physical Sciences*, vol. 6, no. 4, pp. 660-663, 2011, DOI: 10.5897/IJPS10.572

[31] D. R. Smith, S. Schultz, P. Markoš and C. M. Soukoulis, "Determination of Effective Permittivity and Permeability of Metamaterials from Reflection and Transmission Coefficients", in *Physical review B*, vol. 65, no. 19, p. 195104, 2002, DOI: 10.1103/PhysRevB.65.195104

[32] A. Varshney, V. Sharma, T. M. Neebha and N. P. Kumari, "Notch-Band Eliminator Wideband CSRR Loaded Monopole Fractal Antenna for ISM and PCS Communications", in *World Journal of Engineering*", vol. 21, no. 2, 2023, DOI: 10.1108/WJE-08-2022-0333